INTERNATIONAL JOURNAL FOR NUMERICAL METHODS IN FLUIDS, VOL. 7, 247–261 (1987)

ANALYSIS OF SUPERPOSED FLUIDS BY THE FINITE ELEMENT METHOD: LINEAR STABILITY AND FLOW DEVELOPMENT

STERGIOS YIANTSIOS AND BRIAN G. HIGGINS

Department of Chemical Engineering, University of California, Davis, California 95616, U.S.A.

SUMMARY

A Galerkin finite element method is described for studying the stability of two superposed immiscible Newtonian fluids in plane Poiseuille flow. The formulation results in an algebraic eigenvalue problem of the form $\mathbf{A}\lambda^2 + \mathbf{B}\lambda + \mathbf{C} = 0$ which, after transforming to a standard generalized eigenvalue problem, is solved by the QR algorithm. The numerical results are in good agreement with previous asymptotic results. Additional results show that the finite element method is ideally suited for studying linear stability of superposed fluids when parameters characterizing the flow fall outside the range amenable to perturbation methods. The applicability of the finite element method to similar eigenvalue problems is demonstrated by analysing the steady-state spatial development of two superposed fluids in a channel.

KEY WORDS Stability FEM Superposed Fluids

INTRODUCTION

Yih[1] showed by perturbation methods that plane Poiseuille flow of two superposed liquids of different viscosity is unstable to a long wavelength interfacial mode for arbitrary small values of the Reynolds number. Although this instability is related to the jump in viscosity across the interface, its growth rate (or in some cases lack thereof) is dependent in a complicated way on additional parameters such as the layer thickness ratio, the density ratio of the liquids, and whether or not density stratification is stabilizing. Analysing how these parameters as well as others influence the growth rate by perturbation methods is ordinarily limited by the smallness of some appropriate parameter. In Yih's analysis the small parameter was the wave number, whereas in Nakaya and Hasegawa's[2] study the wave number and the Reynolds number were used. Hooper[3] has also made use of a small wave number expansion to determine the stability of superposed fluids. Invariably, because of the attendant tedious algebra, perturbation methods tend to be inefficient for studying flow stability when the number of parameters characterizing the flow becomes large, as is the case considered here.

In this paper we describe a Galerkin finite element method for studying linear stability of plane Poiseuille flow of two superposed liquids. Linear stability is described by an Orr–Sommerfeld equation for each layer. These equations are coupled through the traction and kinematic boundary conditions imposed at the interface separating the two liquids. Our work parallels the recent study of Li and Kot[4] who analysed linear stability of plane Poiseuille flow by the finite element method. There are obvious differences, however. In particular, the presence of a liquid/liquid interface introduces several additional complications in the finite element formulation of the boundary

0271–2091/87/030247–15$07.50

Received 11 November 1985
Revised 10 June 1986

conditions. The complications arise from discontinuities in the eigenfunctions at the interface. A method for handling these discontinuities is described below. We compare our calculated eigenvalues for the most unstable mode with those of Yih, and report new results on flow stability when the disturbance wave number is no longer small and when the fluid layers have disparate thicknesses.

Since our formulation reduces to the single fluid case when appropriate values are assigned to the parameters, we also report on the accuracy of the finite element method for computing eigenvalues of the Orr–Sommerfeld equation for plane Poiseuille flow for modes other than the most unstable (Li and Kot[4] reported results only for the most unstable mode). This is done by comparing our calculated eigenvalues with those of Orszag,[5] which are reputed to be the most accurate available in the literature.

Eigenvalue problems resembling the Orr–Sommerfeld equation also arise in the study of stationary perturbations from rectilinear flow. A detailed analysis of such problems was first given by Wilson[6] who analysed how stationary perturbations from plane Poiseuille flow decay with distance downstream. He solved by asymptotic methods for the limiting cases of small and large Reynolds number the eigenvalue problem that results from linearizing the steady Navier–Stokes equations about the fully developed flow. Bramley and Dennis[7] solved the identical problem using a spectral method (cf. Orszag[5]) for values of the Reynolds number between 0 and 2000, but, as they note, their results are not in full agreement with Wilson's asymptotic expression for the dominant eigenvalue at low Reynolds number.

As a further demonstration of the versatility of the finite element method for analysing eigenvalue problems of the Orr–Sommerfeld type, we discuss also the steady-state spatial development of two-layer flow in a channel. In contrast to the stability problem, the eigenvalue problem for the stationary perturbations is non-linear in the eigenvalue. We compare and discuss our calculated values for the dominant eigenvalue with Wilson's asymptotic results for a single layer.

STABILITY FORMULATION AND FINITE ELEMENT ANALYSIS

The base flow consists of two parabolic profiles non-dimensionalized by the interfacial velocity U_0:

$$U_1 = 1 + a_1 y + b_1 y^2,\ U_2 = 1 + a_2 y + b_2 y^2, \tag{1}$$

where

$$a_1 = \frac{m - n^2}{n + n^2},\ b_1 = -\frac{m + n}{n + n^2},\ a_2 = a_1/m,\ b_2 = b_1/m. \tag{2}$$

The subscript 1 denotes the upper fluid, 2 the lower fluid; m and n are the viscosity and thickness ratios defined in terms of the lower fluid with respect to the upper. The co-ordinate y is made dimensionless with d_1, the layer thickness of the upper fluid: see Figure 1.

To test for stability, the Navier–Stokes equations and boundary conditions are linearized about the base flow (1). A stream function for the disturbance in each layer is assumed to be of the form $f(y)\exp[i\alpha(x - ct)]$, where α is the dimensionless wave number of the disturbance in the flow direction x, and c the dimensionless complex wave speed. When this form for the stream function is substituted into the linearized Navier–Stokes equations, the stability formulation results in two equations of the Orr–Sommerfeld form for the upper and lower fluids respectively:

$$\hat{\phi}^{iv} - 2\alpha^2\hat{\phi}'' + \alpha^4\hat{\phi} - i\alpha R\{(U_1 - c)(\hat{\phi}'' - \alpha^2\hat{\phi}) - U_1''\hat{\phi}\} = 0 \tag{3}$$

$$\hat{\psi}^{iv} - 2\alpha^2\hat{\psi}'' + \alpha^4\hat{\psi} - i\alpha\frac{Rr}{m}\{(U_2 - c)(\hat{\psi}'' - \alpha^2\hat{\psi}) - U_2''\hat{\psi}\} = 0. \tag{4}$$

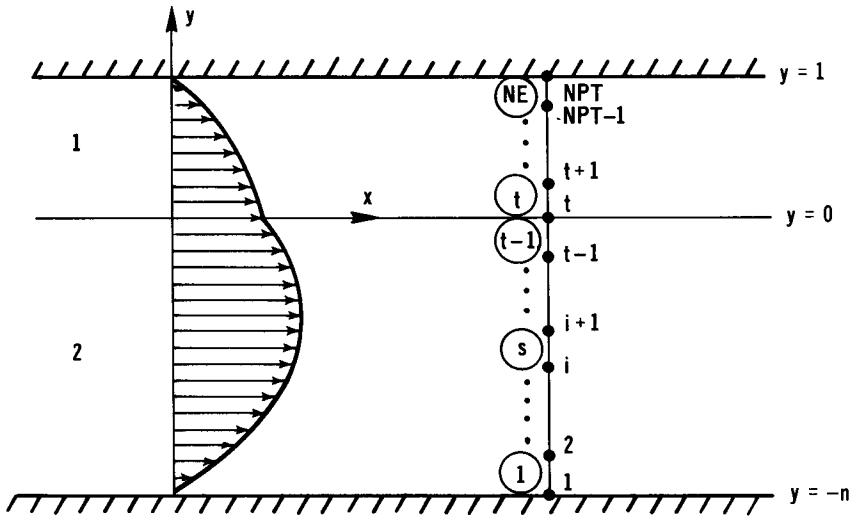

Figure 1. Finite element discretization; S denotes the element

The primes on $\hat{\phi}, \hat{\psi}$ and U_i denote differentiation with respect to the co-ordinate y.

The linearized boundary conditions expressing non-slip at the channel walls and continuity of velocities and stresses at the interface are

$$\hat{\phi}(1) = \hat{\phi}'(1) = 0, \tag{5}$$

$$\hat{\psi}(-n) = \hat{\psi}'(-n) = 0, \tag{6}$$

$$\hat{\phi}(0) = \hat{\psi}(0), \tag{7}$$

$$\hat{\phi}'(0) - \hat{\psi}'(0) = \frac{\hat{\phi}(0)}{c-1}(a_2 - a_1), \tag{8}$$

$$\hat{\phi}'' + \alpha^2\hat{\phi} = m(\hat{\psi}'' + \alpha^2\hat{\psi}), \quad \text{at } y = 0 \tag{9}$$

$$\begin{aligned} &-\mathrm{i}\alpha R[(c-1)\hat{\phi}' + a_1\hat{\phi}] - (\hat{\phi}''' - \alpha^2\hat{\phi}') + 2\alpha^2\hat{\phi}' \\ &+ \mathrm{i}\alpha Rr[(c-1)\hat{\psi}' + a_2\hat{\psi}) + m(\hat{\psi}''' - \alpha^2\hat{\psi}') - 2m\alpha^2\hat{\psi}' \\ &= \mathrm{i}\alpha R(F + \alpha^2 S)\phi/(c-1), \quad \text{at } y = 0. \end{aligned} \tag{10}$$

Here $r = \rho_2/\rho_1$ is the density ratio, $R = \rho_1 U_0 d_1/\mu_1$ the Reynolds number, and $F = (r-1)gd_1/U_0^2$, $S = \sigma/\rho_1 d_1 U_0^2$ the dimensionless groups expressing the effects of gravity g and surface tension σ. Equations (3)–(10) define an eigenproblem for the eigenfunctions $\hat{\phi}(y)$ and $\hat{\psi}(y)$, and the complex eigenvalue $c \equiv c_R + \mathrm{i}c_i$. The flow is linearly unstable when c_i is positive and neutrally stable when $c_i = 0$. The eigenvalue c is a function of r, R, F, S, α, m and r. Additional details concerning the derivation of the above equations are given by Yih.[1]

The finite element equations are determined from the weak formulation of the Orr–Sommerfeld equations, which includes two integrations by parts. The required continuity for the interpolation functions is then C^1. However, with this formulation the first derivatives are discontinuous at the interface (equation (8)), and for this reason it is convenient to treat the two layers separately. The procedure is to split up the interfacial boundary conditions (9) and (10) by introducing additional unknowns. For example, equation (9) is written $m(\hat{\psi}'' + \alpha^2\hat{\psi}) - u_1 = 0$

and $\hat{\phi}'' + \alpha^2\hat{\phi} - u_1 = 0$, where u_1 is an additional unknown. Here we present the treatment for the lower fluid while the one for the upper proceeds along exactly the same steps. In Figure 1 the finite element discretization is presented. The number of nodes in each layer is taken to be the same.

If ψ is the approximation to $\hat{\psi}$, then the residual resulting from (4) at the element level is

$$r_1 = m\psi^{iv} - 2\alpha^2 m\psi'' + \alpha^4 m\psi - i\alpha Rr\{(U_2 - c)(\psi'' - \alpha^2\psi) - U_2''\psi\}$$

for element $s = 1 \to t-1$. Similarly, owing to the discontinuities in the second and third derivatives of the approximation function

$$r_2 = -m\psi'''|_{i-} + m\psi'''|_{i+}$$

and

$$r_3 = m\psi''|_{i-} - m\psi''|_{i+}$$

are the residuals at each node $i = 1 \to t-1$. At the interfacial node t

$$r_4 = m\psi'' + m\alpha^2\psi - u_1$$

and

$$r_5 = -m(\psi''' - \alpha^2\psi') + 2\alpha^2 m\psi' - i\alpha Rr[(c-1)\psi' + a_2\psi] + u_2.$$

The weighted residual statement becomes

$$R_n = \sum_{s=1}^{t-1} \int_{l_s} r_1 N_n \mathrm{d}y + \sum_{i=1}^{t-1} (r_2 N_n)_i + \sum_{i=1}^{t-1} (r_3 N_n')_i + (r_4 N_n')_t + (r_5 N_n)_t = 0. \tag{11}$$

Here l_s is the element length.

Substituting the expressions for the residuals into (11) and integrating by parts twice we get

$$\begin{aligned} R_n = \sum_{s=1}^{t-1} \int_{l_s} \{ & m\psi'' N_n'' + 2\alpha^2 m\psi' N_n' + \alpha^4 m\psi N_n \\ & + i\alpha Rr[U_2\psi' N_n' + U_2'\psi' N_n + \alpha^2 U_2\psi N_n + U_2''\psi N_n] \\ & - i\alpha Rrc[\psi' N_n' + \alpha^2\psi N_n]\} \mathrm{d}y + [2\alpha^2 m\psi' N_n + i\alpha Rr(U_2 - c)\psi' N_n - m\psi''' N_n \\ & + m\psi'' N_n']_1 + [(m\alpha^2\psi - u_1)N_n' + m\alpha^2\psi' N_n + (-i\alpha Rra_2\psi + u_2)N_n]_t = 0. \end{aligned} \tag{12}$$

The approximation for ψ over each element is

$$\psi = \psi_1 N_1 + \psi_2 N_2 + \psi_3 N_3 + \psi_4 N_4 \tag{13}$$

where N_i are cubic Hermite polynomials with the required C^1 continuity and $\psi_2 = \psi_1'$, $\psi_4 = \psi_3'$. In this way we arrive at the element contributions to the weighted residuals which, for elements $s = 2 \to t-2$, have the form

$$\mathbf{R}_n^s = (\mathbf{J} - c\mathbf{M})\boldsymbol{\psi}. \tag{14}$$

Here $\mathbf{J}$ and $\mathbf{M}$ are 4×4 matrices and their final form is given by equations (19) and (20).

At element 1 we choose to satisfy the boundary conditions (6) exactly, and therefore replace the first two equations in (14) for $s = 1$ with $\psi_1 = 0$ and $\psi_2 = 0$.

At element $t-1$, the residuals in (14) for $n = 3$ and 4 are

$$R_3^{t-1} = \sum_{i=1}^{4} (J_{3i} - cM_{3i})\psi_i + m\alpha^2\psi_4 - i\alpha Rra_2\psi_3 + u_2 = 0 \tag{15}$$

$$R_4^{t-1} = \sum_{i=1}^{4} (J_{4i} - cM_{4i})\psi_i + m\alpha^2\psi_3 - u_1 = 0. \tag{16}$$

Following exactly the same steps for the upper fluid we replace the last two residuals at element NE by the exact conditions (5) while the first two residuals at element t have the form

$$R_1^t = \sum_{i=1}^{4} (J_{1i} - cM_{1i})\phi_i - \alpha^2\phi_2 + i\alpha R\left(a_1 + \frac{F + \alpha^2 S}{c-1}\right)\phi_1 - u_2 = 0 \tag{17}$$

$$R_2^t = \sum_{i=1}^{4} (J_{2i} - cM_{2i})\phi_i - \alpha^2\phi_1 + u_1 = 0. \tag{18}$$

Adding equations (15) to (17) and (16) to (18) we eliminate the unknowns u_1 and u_2, and using the boundary conditions (7) and (8) we replace ψ_3 by ϕ_1 and ψ_4 by $\phi_2 - \phi_1(a_2 - a_1)/(c-1)$. with this procedure, matrix changes occur only at element $t-1$. The global matrices are thus easily formed by storing the element matrices in their appropriate positions. The procedure we have adopted of introducing intermediate unknowns u_1 and u_2 is not unique. For example, one could equally well arrive at the same formulation by a straightforward approach of weighting the equations and the interfacial conditions (9) and (10). In this case one would have to introduce four unknowns at node t, namely $\phi(0)$, $\phi'(0)$, $\psi(0)$, $\psi'(0)$, instead of two, resulting in matrices of order 4×6 for elements $t-1$ and t. Subsequently, two of these unknowns could be eliminated by use of (7) and (8) to achieve matrix contraction. The advantage of introducing intermediate unknowns is that it avoids the bookkeeping associated with matrix contraction and, in addition, the method ensures that there are an equal number of unknowns, interpolating functions, and weighting functions. When matrix construction is not carried out, the eigenvalue problem is singular.

To accommodate the inversion of the global matrix $\mathbf{M}$, all the equations are divided by $i\alpha R$ to ensure that $\mathbf{M}$ is real. Hence at the element level we have

$$J_{ij} = \int_{l_s} r\{(U_2 N_i' N_j' + U_2' N_i N_j' + \alpha^2 U_2 N_i N_j + U_2'' N_i N_j) - \frac{i}{\alpha R}(mN_i'' N_j'' + 2\alpha^2 m N_i' N_j' + \alpha^4 m N_i N_j)\}\,dy \tag{19}$$

and

$$M_{ij} = \int_{l_s} r(N_i' N_j' + \alpha^2 N_i N_j)\,dy. \tag{20}$$

The above equations hold for elements $s = 1 \to t-1$, while upon switching to the upper fluid we simply replace U_2 by U_1 and set $r = m = 1$.

At the element $t-1$, the following additions are made to (19):

$$J_{13} = \bar{J}_{13} + (\bar{J}_{14} - cM_{14})(a_1 - a_2)/(c-1)$$

$$J_{23} = \bar{J}_{23} + (\bar{J}_{24} - cM_{24})(a_1 - a_2)/(c-1)$$

$$J_{33} = \bar{J}_{33} + (\bar{J}_{34} - cM_{34})(a_1 - a_2)/(c-1) + a_1 - ra_2 + (F + \alpha^2 S)/(c-1) - i\alpha m(a_1 - a_2)/R(c-1)$$

$$J_{34} = \bar{J}_{34} - i\alpha(m-1)/R$$

$$J_{43} = \bar{J}_{43} + (\bar{J}_{44} - cM_{44})(a_1 - a_2)/(c-1) - i\alpha(m-1)/R$$

where $\bar{J}_{ij}$ is given by (19).

For the case of a single fluid these additions are equal to zero as $a_1 = a_2 = 0$, $m = r = 1$, and $F = S = 0$. The formulation is then identical to that of Li and Kot.[4]

Finally, because the eigenvalue c appears in the denominator of some of the additional terms, we multiply (14) by $c - 1$ so that the matrix eigenvalue problem has the form

$$(\mathbf{A}_1 c^2 + \mathbf{A}_2 c + \mathbf{A}_3)\boldsymbol{\psi} = 0 \tag{21}$$

where $\mathbf{A}_1 = -\mathbf{M}$, $\mathbf{A}_2 = \mathbf{J} + \mathbf{M}$ and $\mathbf{A}_3 = -\mathbf{J}$. This is equivalent to

$$(\mathbf{C}_1 - c\mathbf{C}_2)\bar{\boldsymbol{\psi}} = 0 \tag{22}$$

Where

$$\mathbf{C}_1 = \left|\begin{array}{c|c} -\mathbf{A}_2 & -\mathbf{A}_3 \\ \hline \mathbf{I} & 0 \end{array}\right|, \quad \mathbf{C}_2 = \left|\begin{array}{c|c} \mathbf{A}_1 & 0 \\ \hline 0 & \mathbf{I} \end{array}\right|, \quad \bar{\boldsymbol{\psi}} = \left|\begin{array}{c} c\boldsymbol{\psi} \\ \hline \boldsymbol{\psi} \end{array}\right|.$$

$\mathbf{C}_1$ and $\mathbf{C}_2$ are matrices of the order $n \times n$, where $n = 4NE - 4$. If we further write $(\mathbf{C}_2^{-1}\mathbf{C}_1 - c\mathbf{I})\bar{\boldsymbol{\psi}} = 0$ we have a standard eigenvalue for the matrix $\mathbf{C}_2^{-1}\mathbf{C}_1$ which is complex and non-Hermitian. For the solution of the above problem the QR algorithm was used (e.g. Smith *et al.*[8]).

RESULTS

Yih carried out an asymptotic analysis of (3)–(10) for long wave disturbances ($\alpha \ll 1$) for fluids of equal density and equal layer thickness. He showed that there is an unstable interfacial mode induced by the viscosity difference that persists at arbitrarily small Reynolds numbers.

In Table I and Figure 2 we compare our calculated eigenvalues for the most unstable mode with those reported by Yih.[1] In all the calculations the matrices were of the order 52 × 52. Convergence was tested by increasing the number of elements and the order of matrices accordingly. The viscosity ratio was varied from 2 to 60. The remaining parameters appearing in (3)–(10) were assigned the following values: $R = 1, r = n = 1, F = S = 0$. Table I shows that the real part of the eigenvalue calculated by the finite element method agrees with Yih's value to five decimal places when $\alpha = 0{\cdot}001$. For larger wave numbers, the agreement is not as good. This is to be expected because the error in Yih's value for the real part is $O(\alpha^2)$. For the complex part, Yih gives the formula $c_i = 8\alpha R H_3$, where H_3 is found from his equation (52).[1] In Figure 2 we have plotted H_3 against the viscosity ratio. The discrete data points are our calculations of $c_i/8\alpha R$. These data points when expressed in terms of c_i agree with Yih's values for c_i to at least six decimal places for the studied range $2 < m \leqslant 60$. For example, for $m = 60$ the finite element method gives $c_i = 8{\cdot}269 \times 10^{-5}$, while Yih's result is $c_i = 8{\cdot}26908 \times 10^{-5}$. Additional calculations for $m = 100$ were also found to be in good agreement.

Unlike Yih's perturbation approach, the finite element method (or any other numerical technique for that matter) is not restricted to small wave numbers. In Figure 3 we show the

Table I. The real part of the eigenvalue $c = c_R + ic_i$ for the most unstable mode as a function of the viscosity ratio m. Finite element calculations for $R = 1, r = n = 1, F = S = 0$

Viscosity ratio, m	C_R(Yih[1])	C_R(FEM, $\alpha = 0{\cdot}01$)	C_R(FEM, $\alpha = 0{\cdot}001$)
2	1·060606	1·0606037	1·0606060
4	1·246575	1·2465622	1·2465752
10	1·672199	1·6721406	1·6721986
20	2·060206	2·0600803	2·0602044
40	2·407682	2·4074764	2·4076796
60	2·567665	2·5674167	2·5676625

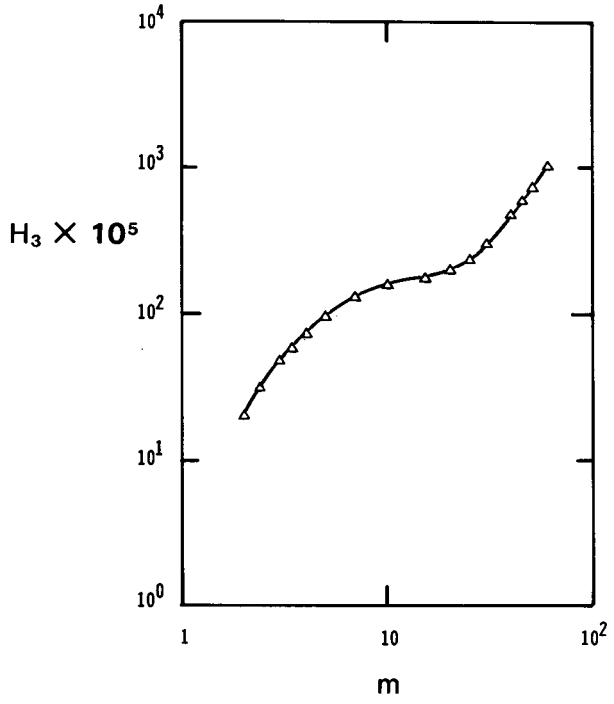

Figure 2. The dependence of Yih's parameter $H_3(\equiv c_i/8\alpha R)$ on the viscosity ratio m. The solid curve is Yih's result; the discrete data points are finite element calculations. The calculations are for $R = 1, r = n = 1, F = S = 0$

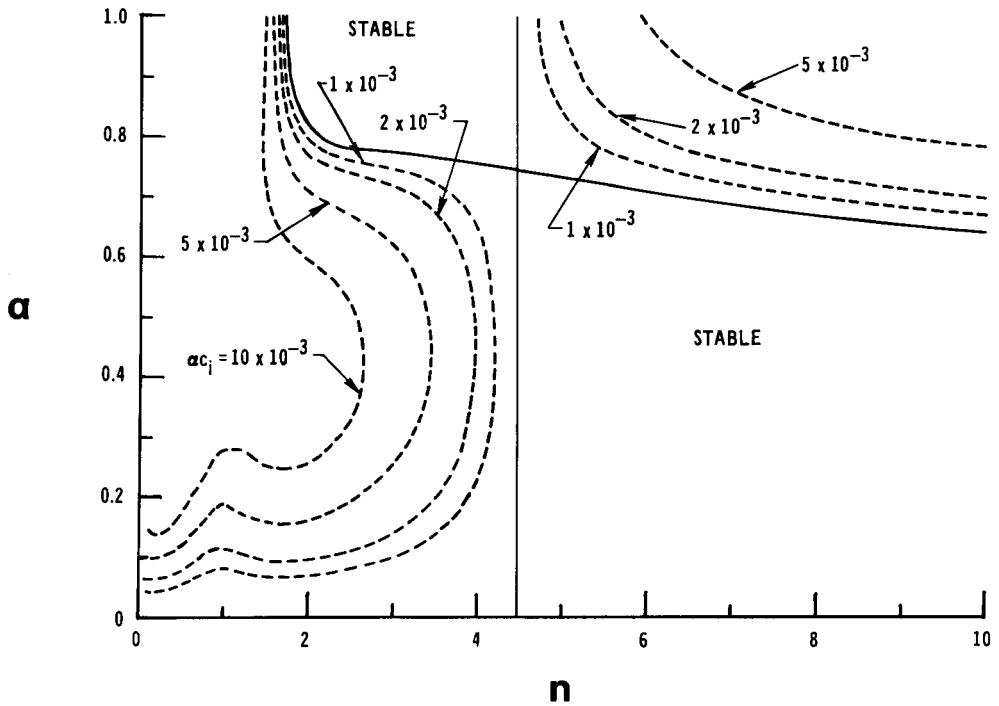

Figure 3. Neutral stability curves $c_i = 0$ (solid lines) and disturbance growth rates αc_i (dashed lines) plotted in the plane of the wave number α and thickness ratio n. The calculations are for $R = 10$, $m = 20$, $r = 1$, $F = S = 0$

Table II. Eigenfunctions corresponding to an unstable interfacial mode; $\alpha = 0{\cdot}5$, $R = 10$, $m = 20$, $n = 3$, $r = 1$, $F = 0$, $S = 0$

y	ϕ or ψ(20 elements)	ϕ or ψ (30 elements)
−3·0	0·000000 + 0·000000 i	0·000000 + 0·000000 i
−2·4	0·052114 + 0·002605 i	0·052114 + 0·002604 i
−1·8	0·189978 + 0·009480 i	0·189978 + 0·009478 i
−1·2	0·396651 + 0·015838 i	0·396651 + 0·015834 i
−0·6	0·666081 + 0·014930 i	0·666082 + 0·014926 i
0·0	1·000000 + 0·000000 i	1·000000 + 0·000000 i
0·2	0·431411 + 0·034945 i	0·431413 + 0·034940 i
0·4	0·127025 + 0·036848 i	0·127026 + 0·036842 i
0·6	0·005660 + 0·022264 i	0·005662 + 0·022260 i
0·8	−0·011139 + 0·006690 i	−0·011139 + 0·006688 i
1·0	0·000000 + 0·000000 i	0·000000 + 0·000000 i

neutral stability curves, $c_i = 0$, plotted in the plane of wave number α and thickness ratio n for $R = 10, m = 20, r = 1, F = S = 0$. The dashed curves are curves of constant growth rate (αc_i) for the unstable mode. It is evident from this plot that the instability mode that Yih found for $n = 1$ is not limited to long waves, and the thickness ratio plays a significant role. When $n > \sqrt{m}$ the plot shows that long waves (small wave numbers) are stable, but short waves are not. The stability results are reversed when $n < \sqrt{m}$, short waves now being stable for certain values of n. The magnitude of the growth rate of the unstable disturbance is also noteworthy. For the parameters chosen by Yih, the growth rate is of order 10^{-8} or less, depending on the magnitude of the wave number, the Reynolds number and viscosity ratio.

With the finite element technique it is now possible to explore the parameter space to find combinations of parameters for which the growth rate of the interfacial mode is large. This will provide the needed information to design experiments beyond the parameter range considered by Kao and Park[9] who were unable to detect with their experimental setup any interfacial instability. A detailed investigation of how the growth rate of the interfacial mode depends on the parameters R, r, m, F and S is discussed elsewhere (Yiantsios and Higgins[10]).

In addition to the calculation of eigenvalues one can easily find the corresponding eigenfunctions. In Table II we tabulate the eigenfunctions corresponding to an interfacial mode. The calculations were carried out using 20 and 30 elements to demonstrate the convergence of the method.

An obvious concern is whether the inherent accuracy of the finite element algorithm is limited by round-off error in the determination of $\mathbf{C}_2^{-1}$. In order to find $\mathbf{C}_2^{-1}$ it is necessary only to invert $\mathbf{M}$ given by (20). The elements of $\mathbf{M}$ are functions of the wave number α, the density ratio r, and the layer thickness ratio n. Note, the last-mentioned parameter enters implicitly through the definition of the shape functions N_i. Whether or not round-off error is an issue in determining $\mathbf{C}_2^{-1}$ is best addressed by calculating the condition number for $\mathbf{M}$:

$$k_2(\mathbf{M}) = \|\mathbf{M}\|_2 \|\mathbf{M}^{-1}\|_2 \tag{23}$$

where $\|\cdot\|_2$ denotes the 2-norm for the matrix (Golub and Van Loan[11]). To calculate k_2 we used the singular value decomposition technique to find the singular values of $\mathbf{M}$ and then used the result that

$$k_2(\mathbf{M}) = \sigma_1/\sigma_2 \tag{24}$$

Table III. Condition number $k_2(\mathbf{M})$

α	$k_2(\mathbf{M})$	
0·001	$0{\cdot}13393 \times 10^4$	
0·01	$0{\cdot}13393 \times 10^4$	
0·1	$0{\cdot}13386 \times 10^4$	$r=1,\quad n=1$
1	$0{\cdot}12897 \times 10^4$	
10	$0{\cdot}13275 \times 10^4$	
100	$0{\cdot}82019 \times 10^4$	
r	$k_2(\mathbf{M})$	
0·1	$0{\cdot}11396 \times 10^5$	
1	$0{\cdot}12897 \times 10^4$	$\alpha=1,\quad n=1$
10	$0{\cdot}11396 \times 10^5$	
n	$k_2(\mathbf{M})$	
0·01	$0{\cdot}12862 \times 10^{10}$	
0·1	$0{\cdot}12676 \times 10^6$	$\alpha=1,\quad r=1$
1	$0{\cdot}12897 \times 10^4$	
10	$0{\cdot}11949 \times 10^4$	
100	$0{\cdot}36239 \times 10^4$	

where σ_1 and σ_2 are the maximum and minimum singular values of $\mathbf{M}$. For details of the procedure, see Golub and Van Loan.[11] In Table III the condition number $k_2(\mathbf{M})$ is tabulated for representative values of α, r and n.

Consider the case analysed by Yih, i.e. $r = n = 1$. We note from Table III that for wave numbers in the range $0{\cdot}001 \leqslant \alpha \leqslant 100, k_2$ is $O(10^3)$. Thus $\mathbf{M}$ is mildly ill-conditioned, and with double precision arithmetic the inversion of $\mathbf{C}_2$ should not be a limiting factor in determining the eigenvalues. That the eigenvalues found by the finite element method are in excellent agreement with Yih's results confirms this.

On the other hand, when the layer thickness ratio is varied, k_2 can become excessive. In particular, as n decreases, k_2 increases, being $O(10^9)$ when $n = 0{\cdot}01$. The reason for this is related to the number of elements and how they are distributed in each fluid layer. In the formulation the co-ordinate y is made dimensionless with d_1. Thus the upper fluid layer has a thickness of unity. Since we have used the same number of elements in each layer, a decrease in n results in the finite element grid in the lower layer becoming disproportionately compressed. When n is decreased by a factor of 100, the grid in the lower layer is clearly not optimal, which apparently causes k_2 to increase. An obvious solution is a variable grid for each layer.

When the density ratio is varied, k_2 changes accordingly, but as Table III shows, k_2 is not overly sensitive to changes in r. Also as the data show k_2 is symmetric about $r = 1$.

It is also of interest to examine whether the finite element method can determine the eigenvalues for additional modes with sufficient accuracy. Unfortunately, in the case of superposed fluids, no detailed comparisons can be made: theoretical results for the stability of superposed fluids are available only for the most unstable mode. However, when $a_1 = a_2, m = r = 1, F = S = 0$ the foregoing finite element formulation describes the stability of plane Poiseuille flow of a single fluid, a case that has been studied extensively in the literature.[12–15] Indeed, Orszag[5] has calculated the most unstable mode and, according to sign and magnitude of the imaginary part, has tabulated the eigenvalues for 31 additional modes when $\alpha = 1$, $R = 10{,}000$. These values are reputed to be the most accurate available in the literature, and serve therefore as a means for evaluating the accuracy of the finite element method presented here.

In Table IV we compare the eigenvalues calculated by the finite element method with those listed by Orszag.[5] When 30 elements were used, the finite element method determines the real part of the most unstable mode to within one part in a thousand. However, the error in the imaginary part is about 24 per cent. Although these results show that there is a significant improvement in the accuracy of the imaginary part for 5 additional modes, the accuracy does become progressively worse for modes beyond 6. When 50 elements were used, the accuracy was improved, and Table IV shows that the imaginary part of the most unstable mode is now within 2 per cent of Orszag's value. This accuracy is maintained or bettered for the next 16 modes.

Since the boundary terms (8)–(10) do not enter into the global matrix $\mathbf{M}$, the condition numbers calculated for $r = n = 1$ also apply in the algorithm to determine the eigenvalues for plane Poiseuille flow. The fact that k_2 was not excessive for the calculations reported in Table IV suggests that the inaccuracy observed in the most unstable mode is not tied directly to round-off error in computing $\mathbf{C}_2^{-1}$. The likely culprit is then $\mathbf{C}_1$, or more precisely $\| \mathbf{C}_1 \|_2 \| \mathbf{C}_2^{-1} \|_2$, which is a measure of the round-off error that will contaminate the QR algorithm (Golub and Van Loan[11]).

As noted Li and Kot,[4] grid refinement in the neighbourhood of the critical layer can help. This is because the dominant eigenfunction of the Orr–Sommerfeld equation is of order $\exp(\pm \alpha R^{1/2})$,[13] and varies rapidly in the neighbourhood of the critical layer. When one is dealing with the eigenvalue problems, mesh refinement does require some care in order to avoid erroneous conclusions, especially when the number of unstable modes is not known *a priori*. This is because different eigenvalues correspond to different eigenfunctions and therefore adaptation of the mesh to a particular eigenfunction is likely to give a poor representation for the rest. This possibility is shown in Table IV. The dominant eigenvalue calculated with a variable mesh, similar to that used by Li and Kot,[4] with 30 elements is more accurate than that calculated using a uniform mesh with either 50 or 30 elements. However, with a variable mesh the second and third eigenvalues are worse and those beyond the third are spurious. In the case of two-layer flow, grid refinement is not as critical (unless $n \ll 1$) as the unstable mode is an interfacial one, that occurs at low Reynolds number.

SPATIAL DEVELOPMENT OF SUPERPOSED FLUIDS

We consider next the *steady-state* spatial development of two-layer flow in a channel. Two immiscible fluid streams are merged in a straight channel. The streams flow side-by-side such that sufficiently far downstream of merging, the flow is fully developed and the interface separating the layers planar. The asymptotic downstream velocity profile is then given by (1). We confine our attention to the region of the flow some distance downstream from the point of merging where the flow, though almost fully developed, is still two dimensional. On the assumption that the deviation from fully developed flow is small, it is permissible to linearize the steady Navier–Stokes equations around (1). The mathematical procedure is described in detail for the single fluid case by Wilson,[6] and for the analogous film flow case by Higgins.[16]

The disturbance stream functions that describe the deviations from fully developed flow are assumed to behave like $\phi(y)\exp(-\alpha x)$ and $\psi(y)\exp(-\alpha x)$ for the two fluids respectively. Substituting expressions of this form into the linearized Navier–Stokes equations results again in an eigenvalue problem where α is now the eigenvalue and not a prescribed wave number. The governing equations can be easily derived from (3)–(10) by letting $c = 0$ and replacing $i\alpha$ by $-\alpha$. It should be noted that the eigenvalues with positive real part (decaying modes) have physical significance. Furthermore, the eigenvalue with the smallest real part is the most interesting since it corresponds to the disturbance mode that persists the longest.

The application of the finite element method proceeds along the same steps as before and the element contributions to the weighted residuals take the form

Table IV. Least stable eigenvalues for plane Poiseuille flow ($\alpha = 1, R = 10{,}000$); Orszag's values are given to five significant figures

Mode	Orszag[5]	EIGENVALUE C 30 elements	30 elements*	50 elements
1.	0·23752 + 0·00373 i	0·23695 + 0·00464 i	0·23744 + 0·00375 i	0·23731 + 0·00379 i
2.	0·96463 − 0·03516 i	0·96455 − 0·03510 i	0·95689 − 0·03151 i	0·96462 − 0·03515 i
3.	0·96464 − 0·03518 i	0·96457 − 0·03512 i	0·96818 − 0·03306 i	0·96463 − 0·03517 i
4.	0·27720 − 0·05089 i	0·27445 − 0·04757 i		0·27673 − 0·05036 i
5.	0·93631 − 0·06320 i	0·93596 − 0·06255 i		0·93626 − 0·06315 i
6.	0·93635 − 0·06325 i	0·93587 − 0·06325 i		0·93629 − 0·06320 i
7.	0·90798 − 0·09122 i	0·89835 − 0·08207 i		0·90782 − 0·09106 i
8.	0·90805 − 0·09131 i	0·87391 − 0·08430 i		0·90788 − 0·09114 i
9.	0·87962 − 0·11923 i	0·91418 − 0·08511 i		0·87924 − 0·11891 i
10.	0·87975 − 0·11937 i			0·87934 − 0·11913 i
11.	0·34910 − 0·12340 i			0·34906 − 0·12279 i
12.	0·41635 − 0·13822 i			0·41570 − 0·13560 i
13.	0·85124 − 0·14723 i			0·85104 − 0·14658 i
14.	0·85144 − 0·14742 i			0·85047 − 0·14664 i
15.	0·82283 − 0·17522 i			0·82129 − 0·17437 i
16.	0·82313 − 0·17547 i			0·82256 − 0·17495 i
17.	0·19005 − 0·18282 i			0·19061 − 0·18206 i
18.	0·79438 − 0·20322 i			0·78683 − 0·19325 i

*Non-uniform mesh.

$$\mathbf{R}^s = (\mathbf{A}_0\alpha^4 + \mathbf{A}_1\alpha^3 + \mathbf{A}_2\alpha^2 + \mathbf{A}_3\alpha + \mathbf{A}_4)\psi, \tag{25}$$

where

$$A_{0ij} = m\int_{l_s} N_i N_j \mathrm{d}y,$$

$$A_{1ij} = rR\int_{l_s} U_2 N_i N_j \mathrm{d}y,$$

$$A_{2ij} = -2m\int_{l_s} N_i' N_j' \mathrm{d}y,$$

$$A_{3ij} = -rR\int_{l_s} (N_i' N_j' U_2 + N_i N_j' U_2' + N_i N_j U_2'')\mathrm{d}y,$$

$$A_{4ij} = m\int_{l_s} N_i'' N_j'' \mathrm{d}y.$$

The above hold for the lower fluid and again m and r are replaced by 1 for the upper fluid. Also the interfacial conditions introduce changes only at the matrices of element $t-1$. The resulting non-linear eigenvalue problem can be easily recast into the standard generalized eigenproblem as described before.

In Table V we show the behaviour of the eigenvalues that become dominant (i.e. those with the smallest real part) for various viscosity ratios and Reynolds numbers. When $m = r = 1$, the eigenvalue problem is identical to that considered by Wilson.[6] At low Reynolds number the dominant eigenvalue, α_0, is complex. As noted in the Introduction, Bramley and Dennis,[7] using a spectral method, were unable to reproduce Wilson's asymptotic results for α_0 at low Reynolds number. The finite element results, on the other hand, are in excellent agreement with Wilson's asymptotic results (see Table V). At high Reynolds number both the spectral and the finite element methods give accurate results. For $R = 1000$ and $m = 1$ we obtain $\alpha_0 = 0{\cdot}02169$ which compares favourably with Wilson's value, viz. $\alpha_0 = 0{\cdot}02168$. (NOTE: our definition for the Reynolds number differs from Wilson's by the factor 2/3.)

For $m > 1$ the dominant eigenvalue need not correspond to a disturbance mode that is dominant at $m = 1$. As the viscosity ratio is increased, Table V shows that a new disturbance mode, whose eigenvalue is real, dominates the spatial development to fully developed flow. The viscosity ratio at which α_1 becomes dominant increases with increasing Reynolds number. At low Reynolds numbers and m close to unity, α_1 is large (relative to unity) and thus plays no role in the spatial development to fully developed flow. Consequently α_1 was not calculated for all values of m and R listed in Table V.

The calculations described above were done using 7 elements in each layer, resulting in sparse matrices of order 104×104. The accuracy of the results obtained with this modest number of elements suggests that the finite element method coupled with an efficient technique for solving sparse eigenvalue problems would be valuable for studying similar kinds of problems.

CONCLUDING DISCUSSION

When superposed fluids become unstable they can do so to an interfacial mode. This mode is unstable at low Reynolds numbers so that the eigenvalue problem is not numerically 'stiff', as is the case in classical linear stability of plane Poiseuille flow of a single fluid. There the flow is unstable to a shear mode that sets in at high Reynolds numbers, and then special care and effort are needed in the numerical algorithm to minimize and control round-off error.

Table V. The dominant modes for spatial development as functions of m and R. Calculations for $r = 1$, $n = 1$, $F = 0$, $S = 0$

	$R = 0{\cdot}1$		$R = 1$		$R = 10$		$R = 100$	
m	α_0	α_1	α_0	α_1	α_0	α_1	α_0	α_1
1	$2{\cdot}0836 \pm 1{\cdot}1341\,i$*	—	$1{\cdot}8978 \pm 1{\cdot}18331$	—	$1{\cdot}1224 \pm 0{\cdot}9230\,i$	5·2319	0·2198†	0·8657
1·2	$2{\cdot}0964 \pm 1{\cdot}1328\,i$	—	$1{\cdot}9225 \pm 1{\cdot}1797\,i$	—	$1{\cdot}1559 \pm 0{\cdot}9520\,i$	4·0891	0·2390	0·9484
1·5	$2{\cdot}1438 \pm 1{\cdot}1326\,i$	5·1274	$1{\cdot}9749 \pm 1{\cdot}1748\,i$	5·2667	$1{\cdot}2108 \pm 0{\cdot}9806\,i$	3·5117	0·2581	1·0473
2	$2{\cdot}2663 \pm 1{\cdot}1631\,i$	3·1892	$2{\cdot}0876 \pm 1{\cdot}1813\,i$	3·3868	$1{\cdot}3047 \pm 1{\cdot}0061\,i$	3·0498	0·2757	1·1319
5	$2{\cdot}4169 \pm 1{\cdot}5645\,i$	1·8309	$2{\cdot}3525 \pm 1{\cdot}5176\,i$	1·8514	$1{\cdot}7853 \pm 1{\cdot}0966\,i$	1·8921	0·2806	1·2675
10	$2{\cdot}3949 \pm 1{\cdot}7037\,i$	1·5801	$2{\cdot}3621 \pm 1{\cdot}6637\,i$	1·5775	$1{\cdot}9151 \pm 1{\cdot}2372\,i$	1·3959	0·2339	0·9083
100	$2{\cdot}3655 \pm 1{\cdot}2829\,i$	1·3630	$2{\cdot}2706 \pm 1{\cdot}6523\,i$	1·2829	$1{\cdot}4631 \pm 0{\cdot}7865\,i$	0·4289	0·2210	0·0447

* Wilson's[6] result for $R \to 0$: $\alpha_0 = 2{\cdot}0834 \pm 1{\cdot}1345\,i$.
† Wilson's[6] result for $R \to \infty$: $\alpha_0 = 0{\cdot}2168$.

The Galerkin finite element method developed here is thus ideally suited for studying the stability of superposed fluids, especially when the parameters characterizing the flow are outside their acceptable range required for conventional perturbation methods. The formulation results in non-linear algebraic eigenvalue problem which can be recast as a conventional eigenvalue problem and solved efficiently by the QR algorithm. One advantage of using the QR algorithm is that additional modes are calculated along with the most unstable mode. The overhead in computing these additional modes is not excessive, however, even for current minicomputers. The present calculations, for example, were done on a VAX 11/780 minicomputer, with the nominal CPU time to calculate 52 eigenvalues being approximately 10 seconds.

In order to implement the QR algorithm it is necessary to compute the inverse of $\mathbf{C}_2$ (equation (22)). We have shown that $\mathbf{C}_2$ is mildly ill-conditioned over much of the parameter space when the same number of elements is used in each layer. However, in situations where $n \ll 1$, appropriate grid refinement in the lower fluid layer is necessary.

The foregoing analysis can be extended in a straightforward manner to analyse the stability of multiple superposed layers. Instead of (21), the formulation results in an algebraic eigenvalue problem of the form

$$(\mathbf{A}_0 c^p + \mathbf{A}_1 c^{p-1} + \ldots . \mathbf{A}_p)\psi = 0 \tag{26}$$

where p denotes the number of layers. Although it is always possible to recast (25) as a generalized algebraic eigenvalue problem, as in (22) (see Wilkinson[17]), the order of the matrix $\mathbf{C}_2$ becomes $(p \times k) \times (p \times k)$, where $k = 2NE - 2$. Thus for large p, the procedure adopted here for solving (22) is likely to be computationally prohibitive. Instead of the QR algorithm approach, it may be more feasible to use Stewart's[18] algorithm for computing invariant subspaces of non-Hermitian matrices.

Finally, eigenproblems similar to the Orr–Sommerfeld system investigated here arise also in the study of linear stability of layered film flow down an incline plane,[19,20] and the asymptotic analysis of downstream development of steady viscocapillary film flows,[16] both of which can be analysed by the method described in this paper. As an example of the latter, we have analysed the spatial development of two-layer flow in a channel. An important application of such problems is the construction of vector Robin conditions for inflow/outflow boundary conditions for use in finite element analysis of coating flows[21] and coating flow stability.[22–24]

ACKNOWLEDGEMENT

This work was supported by National Science Foundation Grant CBT-8505256. The authors thank A. Palazoglu for help with the singular values.

REFERENCES

1. C. S. Yih, 'Instability due to viscosity stratification', *J. Fluid Mech.*, **27**, 337–352 (1967).
2. C. Nakaya and E. Hasegawa, 'Instability of flow of two horizontal fluid layers due to interfacial waves', *J. Phys. Soc. Japan*, **37**, 214–222 (1974).
3. A. P. Hooper, 'Long wave instability of the interface between two viscous fluids: thin layer effects', *Phys. Fluids*, **28**, 1613–1618 (1985).
4. Y. S. Li and S. C. Kot, 'One dimensional finite element method in hydrodynamic stability', *Int. j. numer. methods eng.*, **17**, 853–870 (1981).
5. S. A. Orszag, 'Accurate solution of the Orr–Sommerfeld stability equation', *J. Fluid Mech.*, **50**, 689–703 (1971).
6. S. Wilson, 'The development of Poiseuille flow', *J. Fluid Mech.*, **38**, 793–806 (1969).
7. J. S. Bramley and S. C. R. Dennis, 'The calculation of eigenvalues for the stationary perturbation of Poiseuille flow', *J. Comp. Phys.*, **47**, 179–198 (1982).

8. B. T. Smith, J. M. Boyle, Y. Ikebe, V. C. Klema and C. B. Moler, *Matrix eigensystem routines: EISPACK Guide, 2nd edn*, Springer-Verlag, New York, 1970.
9. T. W. Kao and C. Park, 'Experimental investigation of the stability of channel flows. Part 2. 2-layered co-current flow in a rectangular region', *J. Fluid Mech.*, **52,** 401–423 (1972).
10. S. Yiantsios and B. G. Higgins, submitted to *Phys. Fluids* (1986).
11. G. H. Golub and C. F. Van Loan, *Matrix Computations*, Johns Hopkins University Press, Baltimore, 1983.
12. L. H. Thomas, 'The stability of plane Poiseuille flow', *Phys. Rev.*, **91**(2), 780–783 (1953).
13. B. S. Ng and W. H. Reid, 'An initial value method for eigenvalue problems using compound matrices', *J. Comp. Phys.*, **30,** 125–136 (1979).
14. A. Davey, 'On the numerical solution of difficult boundary value problems', *J. Comp. Phys.*, **35,** 36–47 (1980).
15. J. K. Platten and J. C. Legros, *Convection in Liquids*, Springer-Verlag, Berlin, 1984.
16. B. G. Higgins, 'Downstream development of viscocapillary film flow', *I&EC Fundam.*, **21,** 168–173 (1982).
17. J. H. Wilkinson, *The Algebraic Eigenvalue Problem*, Clarendon Press, Oxford, 1965.
18. G. W. Stewart, 'Simultaneous iteration for computing invariant subspaces of non-Hermitian matrices', *Numer. Math.*, **25,** 123–136 (1976).
19. C. K. Wang, J. J. Seaborg and S. P. Lin, 'Instability of multi-layered liquid films', *Phys. Fluids.*, **21,** 1669–1673 (1978).
20. C. Kobayashi and L. E. Scriven, 'Stability of stratified film flow', paper 46d, AIChE Winter National Meeting, Orlando (1982).
21. S. F. Kistler and L. E. Scriven, 'Coating flow theory by finite element and asymptotic analysis of the Navier–Stokes system', *Int. j. numer. methods fluids*, **4,** 207–229 (1984).
22. N. E. Bixler, *Ph. D. Thesis*, University of Minnesota, Minneapolis, 1982.
23. K. J. Ruschak, 'A three-dimensional linear stability analysis for two-dimensional free boundary flows by the finite element method', *Comp. Fluids*, **11,** 391–401 (1983).
24. D. J. Coyle, C. W. Macosko and L. E. Scriven, 'Liquid flow in a forward roll coater', *TAPPI Proceedings* 1985 Coating Conference, 161–169 (1985).